

Synthesis Control and Characterization of Hydroxyapatite Prepared by Wet Precipitation Process

*Maria Helena Santos, Marise de Oliveira, Luciana Palhares de Freitas Souza,
Herman Sander Mansur*, Wander Luiz Vasconcelos*

*Department of Metallurgy and Materials Engineering Federal University of Minas Gerais
Rua Espírito Santo, 35/206, 30160-030 Belo Horizonte - MG, Brazil*

Received: October 29, 2003; Revised: May 20, 2004

Several techniques have been utilized for the preparation of hydroxyapatite (HA) and other calcium phosphates for the development of biomaterials. It is vital to know the reaction kinetics to be able to control the material obtained by the aqueous solution route. In the present work, HA has been produced by different wet precipitation processes and different experimental conditions. Calcium hydroxide, calcium phosphate, ammonium phosphate and phosphoric acid were used as reagents. The precipitate was dried at 100 °C overnight and then some samples were treated at 900 °C for 2 h. The powder samples were characterized by scanning electron microscopy (SEM), X-ray fluorescence (XRF) and X-ray diffraction (XRD) analyses. SEM photomicrographs showed an aggregate powder, granular to dense and suggested typical columnar particles. Qualitative XRF showed that the main components of HA powders were calcium and phosphorus. Pure HA and other phases according to processing parameters were observed by XRD analysis.

Keywords: *hydroxyapatite, synthesis parameters, X-ray diffraction, bioceramic*

1. Introduction

Considerable research effort has been directed towards the development of artificial bone and teeth that do not cause damage in healthy tissue and can be supplied at any time, in any amount^{1,2}. Synthetic ceramic materials based on calcium phosphate (CaP) particularly in the composition of tricalcium phosphate [TCP-Ca₃(PO₄)₂] and hydroxyapatite [HA-Ca₁₀(PO₄)₆(OH)₂] have extensively been studied and clinically used. Biomaterials research field focus on the synthesis of these ceramics for three decades to applications in orthopedics and dentistry^{1,3-8}. Their use is proposed because they exhibit biological affinity and activity to surrounding host tissues when implanted⁶. Furthermore, according to the literature⁴, calcium phosphates are broadly used in medicine and oral biology due to the apatite-like structure of enamel, dentin and bones, usually called "hard tissues". To date, in spite of availability of several sophisticated characterization techniques for investigation of tooth and bone tissues, their exact composition, distribution of phases and structure remain unresolved⁴. Synthetic Ca-P preparations aim to understand the properties and physicochemical behavior of bio-

logical mineral phases found in human hard tissues because of some order of similarity among them⁵. In addition to that, these materials are also important in the study of biomineralization since they are precursors and major components of bone and teeth⁹. In order to gain insights into the complex structure found in biological mineral phases there would be required a well-defined characterization of the synthetic Ca-P, where the composition, crystallinity and nanostructure have to be properly addressed. These properties play a major role on the bioactivity of Ca-P based materials in terms of enhanced contact areas and degradation⁶. Detailed characterization indicates that an apatite layer is usually formed on the ceramic surface when implanted. This layer consists of carbonate-ion-containing apatite named "bone-like" apatite forming a bond with the human bone¹. These ceramic materials can also be used as coating on implant to improve the biocompatibility^{2,9} and can be injected in bone with non-invasive surgical techniques¹⁰.

Bioactivity of CaP materials is dependent on many factors during the synthesis procedure, such as precursor rea-

*e-mail: hmansur@uol.com.br

Article presented at the II SBPMat, Rio de Janeiro - RJ, 26-29 de Outubro/2003

gents, impurity contents, crystal size and morphology, concentration and mixture order of reagents, pH and temperature. Also, the bioactivity response of Ca-P materials will depend on thermal treatment profile for drying and sintering. These conditions are controlled by synthesis preparation parameters and consequently for each application a specific route is selected^{7,11}.

Based on these considerations, in the present study, we aimed to synthesize calcium phosphate powders from three different routes in aqueous solution, with stoichiometric molar ratio, using different reagent precursors and synthesis parameters. The process parameters evaluated during the synthesis were the temperature and pH of the solution, reagent addition velocity, chemical treatment, thermal treatment and stir speed. The precipitation occurred in aqueous solution and CaP samples were characterized by scanning electron microscopy (SEM), X-ray fluorescence (XRF) and X-ray diffraction (XRD).

2. Experimental procedures

2.1. Samples preparation

Samples were prepared via aqueous precipitation reaction by three synthetic routes with different experimental conditions shown in Table 1.

Route 1 (R1) $10\text{Ca}(\text{OH})_2 + 6\text{H}_3\text{PO}_4 \rightarrow \text{Ca}_{10}(\text{PO}_4)_6(\text{OH})_2 \downarrow + 18\text{H}_2\text{O}$. The 0.5 M calcium hydroxide - $\text{Ca}(\text{OH})_2$ - suspension was prepared using $\text{Ca}(\text{OH})_2$ powder. The suspension was degassed, vigorously stirred and heated for one hour at $40 \pm 2^\circ\text{C}$ temperature. The 0.3 M orthophosphoric acid - H_3PO_4 - solution was dropped into the $\text{Ca}(\text{OH})_2$ suspension at same temperature for approximately one hour. The pH was adjusted by addition of 1 M ammonium hydroxide - NH_4OH

- solution at the end of the precipitation process.

Route 2 (R2) $10\text{Ca}(\text{OH})_2 + 6(\text{NH}_4)_2\text{HPO}_4 \rightarrow \text{Ca}_{10}(\text{PO}_4)_6(\text{OH})_2 \downarrow + 6\text{H}_2\text{O} + 12\text{NH}_4\text{OH}$. The 0.3 M ammonium phosphate - $(\text{NH}_4)_2\text{HPO}_4$ - suspension was dropped into the 0.5 M $\text{Ca}(\text{OH})_2$ suspension prepared as R1 temperature at $40 \pm 2^\circ\text{C}$ for approximately one hour.

Route 3 (R3) $7\text{Ca}(\text{OH})_2 + 3\text{Ca}(\text{H}_2\text{PO}_4)_2 \cdot \text{H}_2\text{O} \rightarrow \text{Ca}_{10}(\text{PO}_4)_6(\text{OH})_2 \downarrow + 15\text{H}_2\text{O}$. The 0.3 M $\text{Ca}(\text{OH})_2$ suspension and 0.12 M calcium hydrogen phosphate hydrate - $\text{Ca}(\text{H}_2\text{PO}_4)_2 \cdot \text{H}_2\text{O}$ - solution were prepared at room temperature and vigorously stirred for ten min. The $\text{Ca}(\text{H}_2\text{PO}_4)_2 \cdot \text{H}_2\text{O}$ solution was added slowly to the $\text{Ca}(\text{OH})_2$ suspension and the mixture was stirred at room temperature for one hour.

On routes two and three the pH was monitored but not corrected. The mixtures were stirred with magnetic stir bar and were aged for 24 h at room temperature. The supernant was decanted. The precipitate was subjected to vacuum filtering using filter paper adapted in a Büchner funnel, repeatedly washed with deionized water (DI) and filtered again. Then, the precipitates were dried at 100°C for 12 h. Deionized water was used to obtain the solutions. The amount of reagents was calculated to make 10 g of HA and each synthesis was repeated two times. Some parameters were varied during the precipitation process and were listed in Table 1.

2.2. Characterization

Some droplets of the mixtures were separated and dried on a glass slide just after total addition mixture. The as-precipitate powders were dispersed in H_2O /ethanol solution and dried on a glass slide too. The samples were coated with a thin layer of gold (Au). The morphology was analyzed on a scanning electron microscope (SEM; JEOL JSM

Table 1. HA sample identifications and experimental conditions.

Sample	Route	Solution adding ratio	Stir speed (magnetic)	Minimum pH	Chemical treatment	Thermal treatment $^\circ\text{C}$
A1	1	6 ml/min	V	7.0	-	-
A2	1	6 ml/min	V	11.5	-	900
A3	1	6 ml/min	V	7.0	-	900*
A4	1	6 ml/min	V	7.0	-	900
A5	1	6 ml/min	V	9.0	yes	900
A6	1	6 ml/min	V	9.0	yes	1100
A7	1	6 ml/min	V	9.5	-	-
A8	2	6 ml/min	V	9.5	-	900
A9	2	6 ml/min	V	9.5	-	900*
A10	3	pouring	S	11.3	-	-
A11	3	pouring	V	11.3	-	900
A12	3	pouring	S	11.3	-	900

* Thermal treatment with fast cooling.

V = vigorous, S = slow

6360 LV) an accelerating voltage ranging from 10 kV to 15 kV. The chemical composition of the samples was determined by X-ray fluorescence (XRF) on Philips PW 2400 equipment. X-ray diffraction (XRD) was employed to identify precipitates and estimate crystallinity on a Philips PW 1710 diffractometer with monochromatized CuK_α radiation and operational tube with voltage and current of 40 kV and 30 mA respectively.

3. Results and discussion

Aqueous solution route was chosen to prepare mixtures of HA because, in contrast to thermal preparation, relatively large amounts of HA can be produced at reasonable cost¹². Furthermore, the only by-product is water and the reaction involves no foreign elements¹¹.

On R1 and R2, the temperature of HA synthesis was maintained at 40 °C and on R3 at room temperature. A higher temperature was used to enhance the reaction kinetics of HA formation and to improve $\text{Ca}(\text{OH})_2$ dissolution, although the HA precipitation also have occurred at room temperature.

The pieces of equipment used in HA synthesis are those usually present in any chemistry laboratory. Regarding to reagents cost, the R1 and R3 were practically similar, while the R2 was 20-25% cheaper.

3.1. SEM analysis

Apatite was present as aggregates, rough, granular to dense and its particles showed different shapes as short and long columns, thick-like plates and needle-like¹³. The aspect of the synthesized powders suggests the typical apatite appearance as shown in Fig.1 and Fig. 2. SEM analysis of the dried droplets is shown in Fig. 3. This photomicrograph suggests columnar shape of the precipitate particles as usually reported^{6,7,11}.

3.2. XRF analysis

The qualitative results of XRF on samples chemical composition of the three routes used can be observed in Table 2. Pure reagents were used for obtaining HA powders. As expected, the major element components were phosphorus (P) and calcium (Ca) that formed the HA synthesized and other trace elements. These trace elements have not interfered in HA synthesis reaction and are most likely that they would not react during the synthesis, staying in the amorphous phase. As they are in the range of parts per million they will not alter the overall biocompatibility response of the material.

3.3. XRD analysis

XRD results of the synthesized precipitates without thermal treatment are shown in Fig. 4. Samples with thermal treatment are shown in Fig. 5 and Fig. 6, following the three different routes. The X-ray diffraction patterns of the HA precipitate synthesized powders were typically HA, in agree-

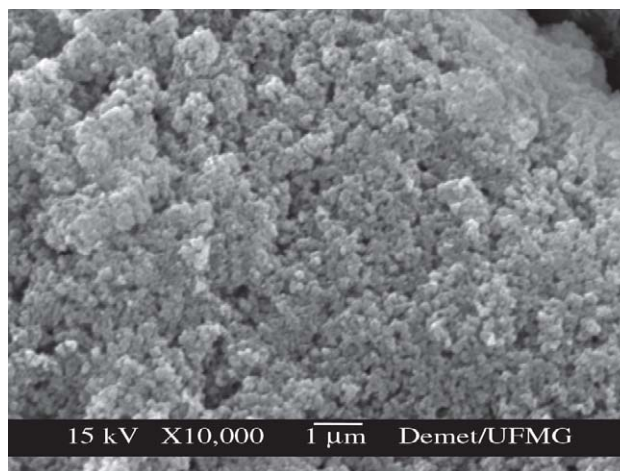


Figure 1. SEM micrograph of sample A1 of synthesized HA powder before thermal treatment.

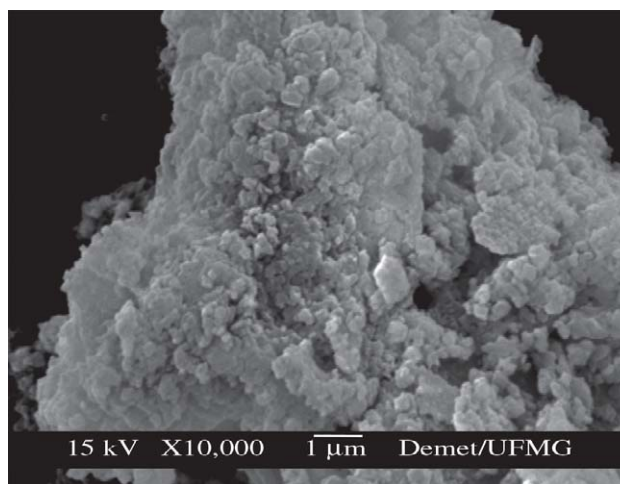


Figure 2. SEM micrograph of sample A4 of synthesized HA powder after thermal treatment.

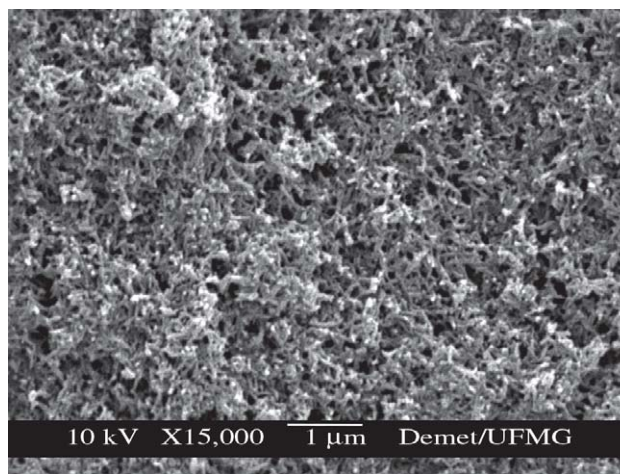
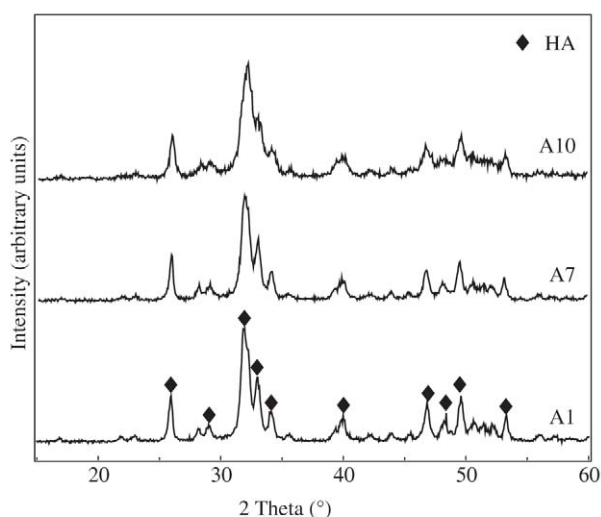


Figure 3. SEM micrograph of as-precipitated HA in a R2 mixture.

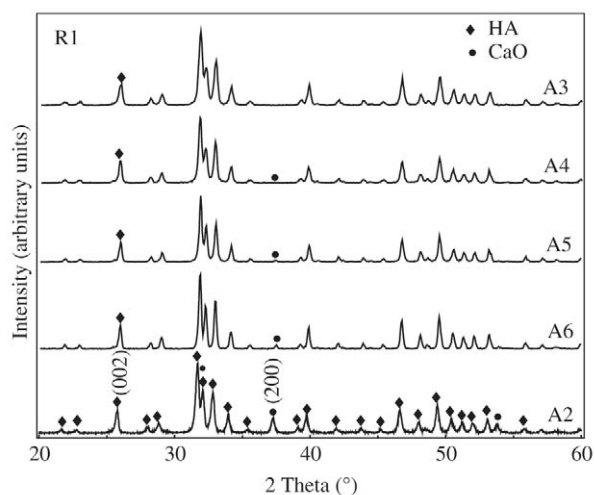
Table 2. XRF of reagents and some HA synthesized powders.

Sample		Element										
		P	Ca	Na	Mg	Si	Sr	Fe	S	Mn	K	Cl
Reagent	Ca(OH) ₂	+	+	*	-	-	*	*	*	*	*	*
	(NH ₄) ₂ HPO ₄	+	+					*	*			
HA	Ca(H ₂ PO ₄) ₂ ·H ₂ O	+	+	*	-	-		*	*		*	
	A1	+	+	*	-	-		*	*			
	A2	+	+	*	-	-	*	*	*		*	*
	A4	+	+	*	-	-	*	*	*			
	A7	+	+	*	-	-	*	*	*			
	A10	+	+	*	-	-		*	*			*
	A12	+	+	*	-	-	*	*	*	*	*	*

Dominant (+), medium (±), low (-) and trace (*) components.

**Figure 4.** XRD patterns of the synthetic precipitate powders after thermal treatment on R1 (sample A1), R2 (sample A7) and R3 (sample A10).

ment with those published in the literature^{7,9,11,14,15}. XRD spectra have characteristic peaks consistent with International Centre for Diffraction Data (ICDD 2001) files for HA. The results in Fig. 4 show the presence of the poorly crystalline HA phase dried at 100 °C and a large amount of amorphous phase for the samples A1, A7 and A10. According to some authors^{7,16} this is a good result because amorphous components would present an improved biodegradation behavior. The low crystallinity characteristic can be reduced by thermal treatment to form a solid entity⁶. This can be confirmed through the comparison of XRD spectra for the samples A1 and A2 (Fig. 4 and 5), A7 and A8 (Fig. 4 and 6), A10 and A12 (Fig. 4 and 6). Differences on the peak widths were observed in these spectra where narrower peaks

**Figure 5.** XRD patterns of the synthetic precipitate powders after thermal treatment on R1.

indicated a more crystalline samples¹⁷.

The aqueous process for the preparation of HA based on R1, Ca(OH)₂ and H₃PO₄, provides a reaction where anions of the phosphate solution (PO₄⁻³) precipitated slowly in calcium metal ions (Ca⁺²) suspension at low pH (Table 1). Thereby, the acid was dropped into alkaline suspension so that the hydroxyl ions present in Ca(OH)₂ suspension are exhausted by H₃PO₄ solution^{18,19}. However, an extra amount of calcium stayed in the precipitated HA, forming a new phase calcium oxide (CaO), besides the hydroxyapatite. Some parameters were compared to observe the presence of this phase. On sample A2 the minimum pH was maintained at 11.5, increasing the CaO phase when compared with a lower minimum pH (7.0) on sample A4 at same con-

ditions (Table 1 and Fig. 5). Sample A5 was subjected to post-chemical treatment, in presence of dilute phosphoric acid solution for 12 h. The association of thermal treatment at 1100 °C and post-chemical treatment was applied in sample A6 (Table 1). These procedures did not show a considerable changes in CaO phase presence (Fig. 5). Then, it was associated the pH 7.0 with a fast cooling after thermal treatment on sample A3. The CaO phase was not present (Fig. 5). It is probable that the fast cooling does not allow the formation of new phases.

The R2 followed the same conditions of R1. The minimum pH 9.5 (Table 1) was monitored without needing to control it by adding alkaline solution most probably due to hydroxide presence. There was a large amount of CaO on the sample A8 that reduced clearly with the fast cooling after thermal treatment as show the spectra of sample A9 (Fig. 6).

On R3, the $\text{Ca}(\text{H}_2\text{PO}_4)_2 \cdot \text{H}_2\text{O}$ solution was added to the $\text{Ca}(\text{OH})_2$ suspension with 0.3 M concentration. The minimum pH 11.3 was monitored (Table 1). Vigorous stirring is the manner of manipulation chosen by the literature¹¹ to achieve perfect mixture of the reagents to obtain HA. Such effect could be confirmed by comparing the spectra of samples A11 and A12 (Fig. 6). Under vigorous stirring, it was observed peaks of pure HA and under slow stirring, biphasic (HA/TCP) material was clearly noted.

The intensity of (200) lattice plan of CaO and (221) lattice plan of TCP on the XRD patterns of precipitated material was used as a direct indicator of its purity as in the Afshar *et al.*¹¹ research. The ratios of the peak intensities on the XRD patterns of CaO/HA ($I_{(200)\text{CaO}}/I_{(002)\text{HA}}$), and TCP/HA

($I_{(221)\text{TCP}}/I_{(002)\text{HA}}$), after thermal treatment, were calculated. The amounts of ($I_{(200)\text{CaO}}/I_{(002)\text{HA}}$) on samples A2, A6, A5, A4 and A3 (Fig. 5) were 0.659, 0.170, 0.079, 0.040 and 0.00; on samples A8 and A9 (Fig. 6) were 1.508 and 0.033 respectively; and the amounts of ($I_{(221)\text{TCP}}/I_{(002)\text{HA}}$) on samples A11 and A12 (Fig. 6) were 0.00 and 2.26, respectively. This calculation can be visualized through the graph in Fig. 7.

Biphasic (HA + TCP) bioceramic has a better bone-bonding ability than pure HA in bony sites and show a new bone formation⁸. The CaO presence does not grant HA smaller biocompatibility²⁰. The control of synthesis parameters commands the developing of HA purity and other phases content in bioceramics.

4. Conclusions

HA was synthesized by three different aqueous precipitation routes. Secondary phase CaO was observed on R1 and R2, and HA + TCP was verified on R3. Process parameters during the HA synthesis, such as pH and thermal treatment have indicated strong influence on the Ca/P phases obtained. The crystallinity of the material was largely increased by thermal treatment and directly influenced the appearing of CaO and TCP secondary phases. The amorphous phase remained in lower amount after thermal treatment.

Acknowledgments

The authors acknowledge the financial support given by CAPES and the technical support received from Microscopy and X-ray laboratories, School of Engineering /UFMG.

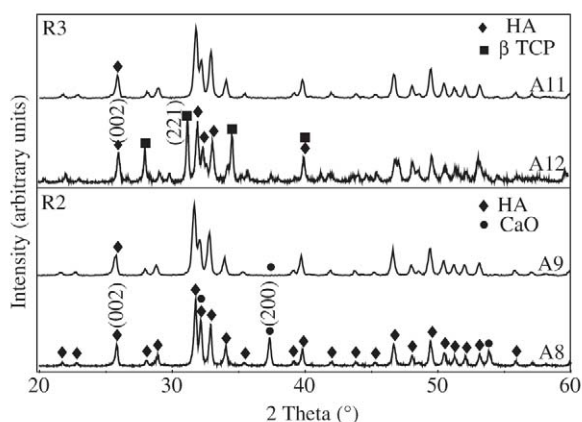


Figure 6. XRD patterns of the synthetic precipitate powders after thermal treatment on R2 (samples A8 and A9) and R3 (samples A11 and A12).

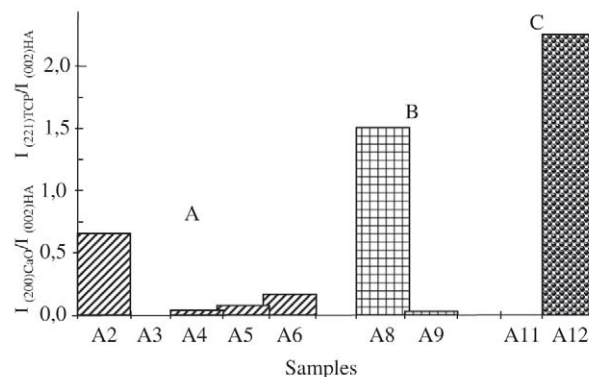


Figure 7. Graphic representation of phase contents measured by the relative intensities of (002) HA lattice planes and (200) CaO lattice planes in XRD patterns of synthesized hydroxyapatite after thermal treatment on R1 samples (A) and R2 samples (B); and (002) HA lattice planes and (221) β -TCP lattice planes on R3 samples (C).

References

1. Kokubo, T., Kim, H.-M., Kawashita, M. *Biomaterials*, v. 24, p. 2161-2175, 2003.
2. Allen, G.C.; Ciliberto, E.; Fragalà, I., Spoto, G. *Nuclear Instruments and Methods in Physics Research B*, v. 116, p. 457-460, 1996.
3. Jones, F.H. *Surface Science Reports*, v. 42, n. 3-5, p. 75-205, 2001.
4. Kikuchi, M.; Itoh, S.; Ichinose, S.; Shinomiya, K.; Tanaka, J. *Biomaterials*, v. 22, n. 13, p. 1705-1711, 2001.
5. Schnettler, R.; Alt, V.; Dingeldein, E.; Pfefferle, H.-J.; Kilian, O.; Meyer, C.; Heiss, C.; Wensch, S. *Biomaterials*, v. 24, p. 4603-4608, 2003.
6. Liou, S.-C.; Chen, S.-Y.; Liu, D.-M. *Biomaterials*, v. 24, p. 3981-3988, 2003.
7. Mavropoulos, E.; Rossi, A.M.; Rocha, N.C.C., Soares, G.A.; Moreira, J.C.; Moure, G.T. *Materials Characterization*, v. 5578, 2003.
8. Li, Y.; Klein, C.P.A.T. *Journal of Materials Science – Materials Medical*, v. 5, p. 263, 1994.
9. Chussei, C.C.; Goodman, D.W. *Analytical Chemistry*, v. 71, n. 1, p. 149-153, 1999.
10. Weiss, P.; Obadia, L.; Magne, D.; Bourges, X.; Rau, C.; Weitkamp, T.; Khairoun, I.; Bouler, J.M.; Chappard, D.; Gauthier, O.; Daculsi, G. *Biomaterials*, v. 24, p. 4591-4601, 2003.
11. Afshar, A.; Ghorbani, M.; Ehsani, N.; Saeri, M.R.; Sorrell, C.C. *Materials & Design*, v. 24, p. 197-202, 2003.
12. Arends, J.; Christoffersen, J.; Christoffersen, M.R.; Eckert, H.; Fowler, B.O.; Heughebaert, J.C.; Nancollas, G.H.; Yesinowski, J.P.; Zawacki, S.J. *Journal of Crystal Growth*, v. 84, p. 515-532, 1987.
13. Schumann, W. *Minerals of the World*, Sterling Publishing Co., New York, 1992.
14. Van Wazer, J.R. *Phosphorus and its compounds*, Interscience, New York, 1958.
15. Chang, M. C.; Ko, C.-C.; Douglas, W.H. *Biomaterials*, v. 24, p. 2853-2862, 2003.
16. Porter, A.E.; Patel, N.; Skepper, J.N.; Best, S.M., Bonfield, W. *Biomaterials*, v. 24, p. 4609-4620, 2003.
17. Kieswetter, K.; Bauer, T.W.; Brown, S.A.; Van Lente, F.; Merrit, K. *Biomaterials*, v. 15, n. 3, p. 4609-4620, 1994.
18. Murry, M.G.S.; Wang, J.; Ponton, C.B.; Marquis, P.M. *Journal of Materials Science*, v. 30, p. 3061-3074, 1995.
19. Osaka, A.; Miura, Y.; Takeuchi, K.; Asada, M.; Takhashi, K. *Journal of Materials Science - Materials Medical*, v. 2, n. 1, p. 51-55, 1995.
20. Monma, H.; Goto, M.; Kajima, H.; Hashimoto, H. *Gypsum and Lime*, p. 202, 1986.